Inorganic Chemistry

ARTICLE

pubs.acs.org/IC

Group 13 Lewis Acid Adducts of $[PCl_2N]_3$

Zin-Min Tun,[†] Amy J. Heston,[†,‡] Matthew J. Panzner,[†] Doug A. Medvetz,[†] Brian D. Wright,[†] Deepa Savant,[†] Venkat R. Dudipala,[†] Debasish Banerjee,[†] Peter L. Rinaldi,[†] Wiley J. Youngs,[†] and Claire A. Tessier[†,*]

[†]Department of Chemistry, The University of Akron, Ohio 44325-3601, United States

[‡]Division of Mathematics and Sciences, Walsh University, North Canton, Ohio 44720-3336, United States

Supporting Information

ABSTRACT: Phosphazene polymers are classically synthesized by the high-temperature, ring-opening polymerization (ROP) of $[PCl_2N]_3$ to give $[PCl_2N]_n$, followed by functionalization of $[PCl_2N]_n$ with different side groups. We investigated the interactions of $[PCl_2N]_3$ with Lewis acids because Lewis acids have been used to induce the high-temperature ROP of $[PCl_2N]_3$. The reactions of $[PCl_2N]_3$ with MX_3 (M = group 13, X = halides), under strict anaerobic conditions gave adducts $[PCl_2N]_3 \cdot MX_3$. Adducts were characterized by X-ray crystallography and multinuclear and variable-temperature NMR studies, and mechanistic understanding of their fluxional behavior in solution was achieved. The properties of the $[PCl_2N]_3 \cdot MX_3$ adducts at or near room temperature strongly suggests that such adducts are not involved directly as intermediates in the high-temperature ROP of $[PCl_2N]_3$.

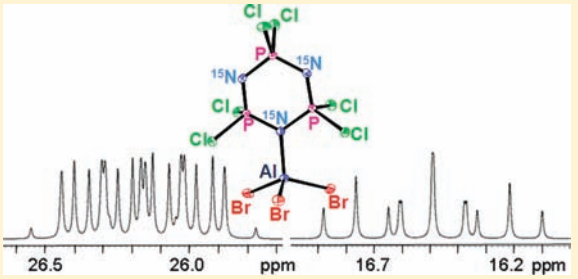

INTRODUCTION

An important route to phosphazene polymers involves the ring-opening polymerization (ROP) of $[PCl_2N]_3$ to the parent polymer $[PCl_2N]_n$, which is then functionalized.[1] The mechanism of the ROP, which can take place both with or without a catalyst or initiator, is still the subject of some controversy.[1−3] We have embarked on a project to better understand the species that have been proposed as intermediates in the ROP of $[PCl_2N]_3$. Chart 1 shows four such species. Phosphazenium ion **1** has been proposed as intermediate in the most commonly accepted mechanism of the uncatalyzed ROP.[1] Though species **1** never has been isolated, a base-stabilized hexacation, in which all six chlorides of $[PCl_2N]_3$ were ionized, has recently been reported.[4] The phosphazenium ion **2** and the isomeric adduct **3** have been proposed as intermediates in the Lewis-acid (LA) initiated ROP.[5] In fact, compounds of structure **3**, in which the LA is a silyl cation are catalysts or initiators for the ROP and allow it to proceed at room temperature.[6] Ion **2** can be viewed as a stabilized analog of **1** in which the Cl^- anion is replaced by a more weakly coordinating anion ($LA(Cl)^-$). Interestingly, **2** also has been proposed as an intermediate in the $AlCl_3$-catalyzed Friedel−Crafts substitution of $[PCl_2N]_3$.[7] Cation **4** has been proposed in an alternative mechanism of the ROP to explain that small quantities of water are required in the ROP.[2,3] Structure **4** is simply a variant of **3**, in which the Lewis acid is H^+.

It has been known for a long time that the nitrogen atoms of $[PCl_2N]_3$ are weak Lewis and Brönsted bases.[8] Though a number of reactions between $[PCl_2N]_3$ and Lewis acids had been reported,[9,10] it was only recently that such compounds have been characterized well enough to know whether their structures are **2**−**4** or other possibilities. We communicated our studies, including crystal structures, of the adducts formed from the reactions of $[PCl_2N]_3$ and the Lewis acids $AlCl_3$, $GaCl_3$ and H^+.[11] Since then, crystal structures of adducts of Ag^+, $SiMe_3^+$, Me^+, and H^+ have been reported.[6,12] All these recent studies are consistent with the structure **3** or its variant **4**. Herein, we describe complete characterization of the adducts $[PCl_2N]_3 \cdot MX_3$, including variable-temperature NMR, dynamic NMR, multinuclear NMR, and X-ray crystallographic studies.

EXPERIMENTAL SECTION

General Procedures. All manipulations were performed under argon, nitrogen, or vacuum using standard anaerobic techniques.[13,14] The vacuum line had an ultimate capability of 2×10^{-4} Torr. The atmosphere of the glovebox was routinely checked by a light-bulb test, and the oxygen and moisture content inside the box was kept between 1 and 5 ppm. All glassware was dried in the oven overnight (∼120 °C). Reaction apparati were either assembled hot and were immediately subjected to vacuum on the Schlenk line or the hot glassware was placed in the port of the glovebox and immediately evacuated before assembly in the glovebox. The glassware used for the experiments was made with virtually greaseless Fisher−Porter Solv-seal glass joints. High vacuum valves on the flasks were purchased from Kimble−Kontes. Infrared spectra were collected on a Nicolet Nexus 870 Fourier transform spectrometer as Nujol mulls. Nujol mulls were prepared in the glovebox. The mulls were placed in a desiccator and were not exposed to air until they were placed on the spectrometer.

Materials. Hexane (Fisher) and methylene chloride (Fisher) were purified by using the PurSolv solvent purification system made by

Received: May 20, 2011
Published: August 18, 2011

Chart 1. Proposed Intermediates in the ROP of $[PCl_2N]_3$

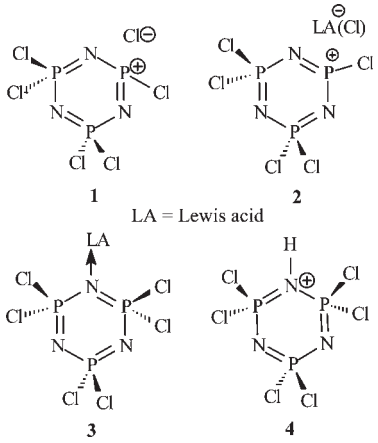

Innovative Technologies. Deuterated methylene chloride (99.9%) and deuterated chloroform (99.8%) were purchased from Cambridge Isotopes, distilled three times over freshly activated 4 Å molecular sieves, and stored under argon in foil-wrapped storage tubes in the glovebox. C_6D_6 (Aldrich) was dried three times with freshly activated 4 Å molecular sieves and stored under argon. Nujol was dried over molecular sieves and stored in the glovebox. $^{15}NH_4Cl$ (Cambridge Isotopes) and PCl_5 (Aldrich) were used as received. The nitrogen isotope composition in the $^{15}NH_4Cl$ salt (97.02% ^{15}N and 2.98% ^{14}N) was determined using FAB mass spectrometry. The synthesis of $[PCl_2{}^{15}N]_3$ was conducted as described in the literature with minor modifications including the use of the labeled $^{15}NH_4Cl$. After careful sublimation at 60 °C for 17 days, the ^{31}P NMR spectrum showed 98% $[PCl_2N]_3$ and 2% $[PCl_2N]_4$. $AgCB_{11}H_6Br_6$ (Strem) and the Aldrich products, $BiCl_3$, BBr_3, $B(C_6F_5)_3$, BCl_3, PCl_5, CS_2, $AgSO_3CF_3$, triflic acid, and $AgCB_{11}H_6Br_6$ (Strem) were used as received. $AlCl_3$, $AlBr_3$, $InCl_3$ (Aldrich), and $GaCl_3$ (Strem) were purified via sublimation and stored in the glovebox.

NMR Spectroscopy. NMR samples were prepared in the glovebox, and all NMR tubes were flame-sealed under vacuum. In order to minimize the presence of protonated impurities, NMR samples of $[PCl_2N]_3 \cdot MX_3$ were made within 24 h of the adduct's preparation. The NMR spectra were either taken *immediately* after the NMR samples were prepared or the tube was kept frozen (liquid nitrogen) until the spectra were taken. Routine NMR spectra were obtained using Varian Gemini 300 MHz or INOVA 400 MHz instruments at 25 °C. VT NMR data were obtained on a Varian INOVA 400 MHz NMR spectrometer with a 5 mm switchable probe. Proton NMR spectra were referenced to the residual proton resonance in the deuterated solvent, and the ^{13}C NMR spectra were referenced to the solvent peak at 128.39 (3) ppm for C_6D_6, 54.00 (5) ppm for CD_2Cl_2, and 20.4(7) ppm (CD_3 resonance) for toluene-d_8. External references were used for the other nuclei: 0.15 M H_3PO_4 solution in deuterated solvent (0 ppm) for the ^{31}P spectra, 0.2 M NH_4NO_3 solution in deuterated water (0 ppm) for the ^{15}N spectra, and 1 M $AlCl_3$ solution in deuterated water (0 ppm) for the ^{27}Al spectra. ^{15}N and ^{31}P NMR were collected with continuous decoupling for NOE. The $^{31}P-^{31}P$ homonuclear J-resolved spectrum (homo2DJ) of $[PCl_2{}^{15}N]_3 \cdot AlBr_3$ was acquired at −60 °C using an 8.1 μs ^{31}P $\pi/2$ pulse width, 0.365 s acquisition time, and 1.5 s relaxation delay. A 2271 Hz spectral window was used for the direct (^{31}P) dimension, whereas a 150 Hz window was used for the indirect (J) dimension. For each of the 256 t_1 increments in the indirect detection axis (f1), 32 transients were averaged. The data were extended to 768 points in the f1 dimension using linear prediction, zero filled to provide a 4096 × 4096 data matrix, and processed using shifted sinebell weighting functions.

X-ray Crystallography. In the glovebox, crystals were put into Paratone oil on a slide. The slide was transported from the glovebox to the instrument in a desiccator that was wrapped in aluminum foil. The crystals were immediately mounted in low light, and the data collection took place with the laboratory lights turned off.

Crystal structure data sets were collected on a Bruker Apex CCD diffractometer with graphite-monochromated Mo Kα radiation (λ = 0.71073 Å). Unit cell determination was achieved by using reflections from three different orientations. An empirical absorption correction and other corrections were done using multiscan SADABS. Structure solution, refinement, and modeling were accomplished using the Bruker SHELXTL package.[15] The structures were obtained by full-matrix least-squares refinement of F^2 and the selection of appropriate atoms from the generated difference map. Crystal data and structure refinement for $[PCl_2N]_3 \cdot AlBr_3$ are given in Table 1 and those for $[PCl_2N]_3 \cdot AlCl_3$ and $[PCl_2N]_3 \cdot GaCl_3$ are given in the Supporting Information.

Preparations of $[PCl_2{}^{15}N]_3 \cdot MX_3$ and $[PCl_2N]_3 \cdot MX_3$. $[PCl_2N]_3 \cdot AlCl_3$ and $[PCl_2N]_3 \cdot GaCl_3$ were synthesized following our published procedures.[11] $[PCl_2{}^{15}N]_3 \cdot AlBr_3$ and $[PCl_2N]_3 \cdot AlBr_3$ were synthesized with a slight modification of the said procedures by using $AlBr_3$ instead. In order to avoid protonated impurities, high vacuum line and glovebox techniques were used as much as possible instead of the Schlenk line, and the above-mentioned precautions were taken in the preparation of NMR samples. *Because the three $[PCl_2N]_3 \cdot MX_3$ (MX_3 = $AlCl_3$, $AlBr_3$ or $GaCl_3$) adducts are light sensitive, exposure to light was minimized throughout all phases of the work.* For $AlCl_3$ and $AlBr_3$, the adduct syntheses can be done using either hexane or CH_2Cl_2 as solvent. However the adduct formation was observed only in hexane for $GaCl_3$. ***Caution***: *It has been reported that $AlBr_3$ reacts exothermically with CH_2Cl_2.*[17,18] We have never observed such a reaction in these systems when following our published procedures.[11]

$[PCl_2{}^{15}N]_3 \cdot AlBr_3$: Yield 83%. Mp: 177−178 °C. IR (Nujol mull cm^{-1}): 1301 (m), 1236 (m), 1194 (s), 1173 (vs), 1084 (w), 1020 (w), 942 (m), 851 (m), 757 (m), 722 (m), 688 (w), 667 (w), 640 (m), 626 (m), 609 (s), 525 (s). Anal. Calcd. for $[PCl_2{}^{15}N]_3 \cdot AlBr_3$: P, 15.05%; Al, 4.37%. Found: P, 15.13%; Al, 4.55%. ^{31}P NMR (C_6D_6): 27.1 ppm (b, s), 16.8 ppm (b, s). ^{15}N NMR (C_6D_6): 93.3 ppm (m, unresolved). ^{27}Al NMR (C_6D_6): 94.0 ppm (b, s, fwhm = 423 Hz).

$[PCl_2N]_3 \cdot AlBr_3$: Yield: 87%. Mp: 174−175 °C. ^{31}P NMR ($CDCl_3$) at 0 °C: δ 26.7 ppm (d), 16.7 ppm (t). ^{27}Al NMR ($CDCl_3$) at 30 °C: δ 100.6 ppm (b, s).

$[PCl_2N]_3 \cdot AlCl_3$: Yield: 90%. Mp: 128−130 °C. ^{31}P NMR ($CDCl_3$) at 0 °C: δ 26.8 ppm (d), 16.6 ppm (t). ^{27}Al NMR ($CDCl_3$) at 30 °C: δ 100.9 ppm (b, s).

$[PCl_2N]_3 \cdot GaCl_3$: Yield: 80%. Mp: 126−127 °C. ^{31}P NMR ($CDCl_3$) at −55 °C: δ 25.28 ppm (d), δ 16.08 ppm (t).

Attempted Preparations of $[PCl_2N]_3$ Adducts with other Lewis Acids. Using conditions similar to our published procedures,[11] we attempted to make adducts with $BiCl_3$, BBr_3, $B(C_6F_5)_3$, BCl_3, PCl_5, CS_2, $AgSO_3CF_3$, and triflic acid in hexane or with $AgCB_{11}H_6Br_6$ in toluene. In all cases, only unreacted starting materials were obtained.

RESULTS AND DISCUSSION

The reaction of MX_3 (MX_3 = $AlCl_3$, $AlBr_3$ or $GaCl_3$) and $[PCl_2N]_3$ with rigorous exclusion of water gave 1:1 complexes as colorless crystals (eq 1). Hexane was a useful solvent for the preparation of all three adducts, but only the $AlCl_3$ and $AlBr_3$ adducts could be prepared in CH_2Cl_2. A published assertion that the adduct $[PCl_2N]_3 \cdot GaCl_3$ could not be prepared may have been due to the use of an inappropriate solvent.[16] $[PCl_2N]_3 \cdot AlBr_3$ had been prepared in nonpolar CS_2, and our IR spectral data is in agreement with the data in this report.[9a] Contrary to a previous report,[9i] we were unable to isolate

Table 1. Crystal Data and Structure Refinement for $[PCl_2N]_3 \cdot AlBr_3$

empirical formula	Al Br3 Cl6 N3 P3	
formula weight	614.35	
temperature	100(2) K	
wavelength	0.71073 Å	
crystal system	monoclinic	
space group	$P2(1)/m$	
unit cell dimensions	a = 10.8919(12) Å	α = 90°
	b = 12.1067(14) Å	β = 91.898(2)°
	c = 12.1387(14) Å	γ = 90°
volume	1599.8(3) Å^3	
Z	4	
density (calculated)	2.551 Mg/m^3	
absorption coefficient	8.898 mm^{-1}	
F(000)	1144	
crystal size	0.15 × 0.07 × 0.03 mm^3	
theta range for data collection	1.68−26.30°	
index ranges	$-13 \le h \le 13$, $-14 \le k \le 15$, $-15 \le l \le 15$	
reflections collected	12824	
independent reflections	3402 [R(int) = 0.0243]	
completeness to theta =26.30°	99.9%	
absorption correction	semiempirical from equivalents	
max and min transmission	0.766 and 0.547	
refinement method	full-matrix least-squares on F^2	
data/restraints/parameters	3402/0/163	
goodness-of-fit on F^2	1.043	
final R indices [I > 2sigma(I)]	R1 = 0.0202, wR2 = 0.0450	
R indices (all data)	R1 = 0.0248, wR2 = 0.0465	
largest diff. peak and hole	0.490 and −0.348 e Å^{-3}	

compounds of other stoichiometries with $AlCl_3$. However, the previous work was done in air. No adducts other than the 1:1 could be isolated with $AlBr_3$.

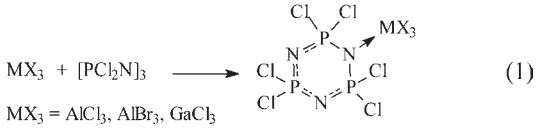

(1)

The three $[PCl_2N]_3 \cdot MX_3$ adducts had melting points that were different from those of their respective reagents. The adducts are insoluble in hexane, have some solubility in aromatic solvents, and have good solubility in CH_2Cl_2 and $CHCl_3$.

The three $[PCl_2N]_3 \cdot MX_3$ adducts were water and light sensitive in solution and in the solid state. All NMR spectra showed the presence of traces of protonated impurities. The NMR tubes were prepared in a glovebox (whose atmosphere was regularly tested) and flame-sealed under vacuum. However, it appears that the flame-sealing of the tubes liberates water from the glass walls, which gives rise to the protonated impurities. The NMR spectra were either taken *immediately* after the NMR samples were prepared or the tube was kept in liquid nitrogen until the spectra were taken. The combination of chloromethanes with $AlCl_3$ or $AlBr_3$ gives a very reactive species, sometimes called superelectrophiles, which may account for the higher prevalence of impurities in CH_2Cl_2 and $CHCl_3$.[17] It has been reported that $AlBr_3$ reacts exothermically with CH_2Cl_2 to give $AlCl_3$ and CH_2BrCl.[18] We observed no such reactions of $[PCl_2N]_3 \cdot AlBr_3$ with CH_2Cl_2.

The reactions of $[PCl_2N]_3$ with other Lewis acids were examined. It is clear that only stronger Lewis acids[19] form complexes with the weak base $[PCl_2N]_3$. A BCl_3 adduct has been proposed as an intermediate in the BCl_3 initiated ROP of $[PCl_2N]_3$.[5] We could not isolate such an adduct, even in hexane. Adducts of $[PCl_2{}^{15}N]_3$ or $[PCl_2N]_3$ could not be isolated with the Lewis acids BBr_3, $B(C_6F_5)_3$, $InCl_3$, $BiCl_3$, PCl_5, $AgSO_3CF_3$, and $Ag(CB_{11}H_6Br_6)$. The latter reaction was conducted in toluene because of the low solubility of the silver reagent in hexane. A low-resolution crystal structure of the product showed a silver ion that was complexed to toluene rather than to $[PCl_2{}^{15}N]_3$. Because a reaction that involved SbF_5 and $[PCl_2{}^{15}N]_3$ gave evidence by NMR spectroscopy for the formation of PF_2 groups, reactions of $[PCl_2N]_3$ with other fluoride containing Lewis acids were not examined. There is disagreement in the literature on whether a reaction takes place between $[PCl_2N]_3$ and $SbCl_5$ at room temperature.[9a,b] Even after repeated attempts that included the use of freshly distilled $SbCl_5$ in an all glass vessel, the only complex we were able to isolate from the reaction of $SbCl_5$ with $[PCl_2N]_3$ was of structure **4** (Chart 1), which forms in the presence of water or HCl. This will be described in an upcoming publication.

X-ray Crystal Structures. The thermal ellipsoid plot for the crystal structure of $[PCl_2N]_3 \cdot AlBr_3$ is shown in Figure 1, and similar plots for $[PCl_2N]_3 \cdot AlCl_3$ and $[PCl_2N]_3 \cdot GaCl_3$ are given in the Supporting Information. Selected distances and angles of the three $[PCl_2N]_3 \cdot MX_3$ are given in Table 2. The asymmetric units of $[PCl_2N]_3 \cdot AlCl_3$ and $[PCl_2N]_3 \cdot AlBr_3$ contain half of two different molecules, whereas that of $[PCl_2N]_3 \cdot GaCl_3$ contains two different molecules. In each case, the only statistically significant differences between the different molecules are in the dihedral angles of the nonplanar rings.

The three $[PCl_2N]_3 \cdot MX_3$ molecules have structure **3** (Chart 1). The Al−N bonds of $[PCl_2N]_3 \cdot AlCl_3$ (1.983(3) and 1.970(3), average = 1.977 Å) are shorter than those of $[PCl_2N]_3 \cdot AlBr_3$ (1.995(3) and 1.992(3), average = 1.994 Å). The latter distance is only slightly shorter than the Ga−N bonds of $[PCl_2N]_3 \cdot GaCl_3$ (2.050(3) and 2.044(3), average = 2.047 Å). The distances between group 13 and the nitrogen atoms are in the range of dative bonds (M = Al, 1.94−2.10 Å;[20] M = Ga, 1.95−2.20 Å[16,21] in four-coordinate compounds). When compared to distances in other MCl_3 adducts of nitrogen-containing bases, the M−N bonds of the three $[PCl_2N]_3 \cdot MCl_3$ (M = Al, Ga) are relatively long and suggest weaker interactions. In addition, the Al−N distances can be compared to those computed for $[PH_2N]_3 \cdot AlF_3$ at 1.901 Å and for $[P(OH)_2N]_3 \cdot AlF_3$ at 1.896 or 1.949 Å (depending on the level of theory).[22] In these two adducts, both the Lewis acid and the Lewis base are stronger than those in the three $[PCl_2N]_3 \cdot MX_3$ reported herein.

The phosphazene rings in the $[PCl_2N]_3 \cdot MX_3$ adducts have slight chair-like structures in which the nitrogen atom bound to the group 13 element (N(1)) and the opposite phosphorus atom

dx.doi.org/10.1021/ic201075z |*Inorg. Chem.* 2011, 50, 8937–8945

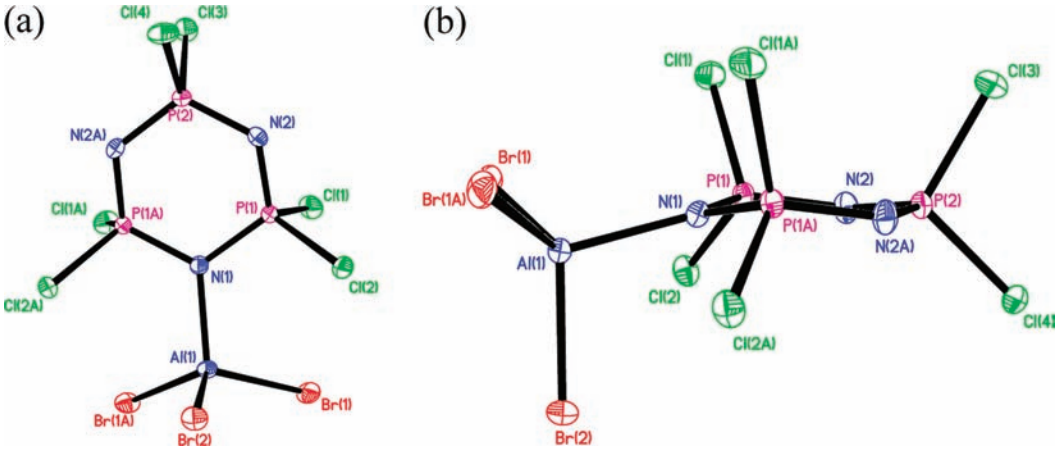

Figure 1. (a) Thermal ellipsoid plot for the crystal structure of $[PCl_2N]_3 \cdot AlBr_3$. (b) Chair-like structure of $[PCl_2N]_3 \cdot AlBr_3$.

Table 2. Selected Distances (Å) and Angles in $[PCl_2N]_3$, $[PCl_2N]_3 \cdot AlBr_3$, $[PCl_2N]_3 \cdot AlCl_3$, and $[PCl_2N]_3 \cdot GaCl_3$

$[PCl_2N]_3$[a]		$[PCl_2N]_3 \cdot AlBr_3$		$[PCl_2N]_3 \cdot AlCl_3$		$[PCl_2N]_3 \cdot GaCl_3$	
		Al(1)−N(1)	1.995(3)	Al(1)−N(1)	1.983(3)	Ga(1)−N(1)	2.050(3)
		Al(2)−N(4)	1.992(3)	Al(2)−N(3)	1.970(3)	Ga(2)−N(4)	2.044(3)
		P−N distances that flank the nitrogen atom that is bound to MX_3					
		P(1)−N(1)	1.6527(15)	P(1)−N(1)	1.6515(15)	P(1)−N(1)	1.644(3)
		N(1)−P(1)#1	1.6527(15)	N(1)−P(1)#1	1.6515(15)	P(2)−N(1)	1.650(3)
		N(4)−P(3)#2	1.6520(15)	N(3)−P(3)	1.6527(14)	P(4)−N(4)	1.646(3)
		P(3)−N(4)	1.6520(15)	P(3)#1−N(3)	1.6527(14)	P(5)−N(4)	1.644(3)
P−N distances				Other P−N bond distances			
P(2)−N(1)	1.575(3)	P(1)−N(2)	1.562(2)	P(1)−N(2)	1.561(2)	P(1)−N(3)	1.567(3)
P(2)−N(2)	1.575(4)	P(2)−N(2)#1	1.576(2)	P(2)−N(2)#1	1.572(2)	P(2)−N(2)	1.567(3)
P(1)−N(2)	1.575(4)	P(2)−N(2)	1.576(2)	P(2)−N(2)	1.572(2)	P(3)−N(2)	1.571(3)
		P(3)−N(3)	1.563(2)	P(3)−N(4)	1.560(2)	P(3)−N(3)	1.576(3)
		P(4)−N(3)	1.577(2)	P(4)−N(4)	1.574(2)	P(4)−N(6)	1.562(3)
		P(4)−N(3)#2	1.577(2)	P(4)−N(4)#1	1.574(2)	P(5)−N(5)	1.563(4)
						P(6)−N(6)	1.568(4)
						P(6)−N(5)	1.576(4)
				P−N−P angles for N bound to MX_3			
		P(1)#1−N(1)−P(1)	117.01(17)	P(1)#1−N(1)−P(1)	117.68(16)	P(2)−N(1)−P(1)	118.3(2)
		P(3)#2−N(4)−P(3)	117.85(16)	P(3)−N(3)−P(3)#1	117.18(15)	P(4)−N(4)−P(5)	118.1(2)
P−N−P angles				Other P−N−P angles			
P(2)−N(1)−P(2′)	121.2(4)	P(1)−N(2)−P(2)	123.77(17)	P(1)−N(2)−P(2)	125.33(13)	P(1)−N(3)−P(3)	123.9(2)
P(1)−N(2)−P(2)	121.5(3)	P(3)−N(3)−P(4)	124.71(14)	P(3)−N(4)−P(4)	124.48(13)	P(2)−N(2)−P(3)	124.2(2)
						P(5)−N(5)−P(6)	124.7(2)
						P(4)−N(6)−P(6)	125.0(2)
N−P−N angles				N−P−N angles			
N(2)−P(1)−N(2′)	118.3(2)	N(2)−P(1)−N(1)	116.48(12)	N(2)−P(1)−N(1)	116.48(11)	N(2)−P(2)−N(1)	116.07(18)
N(1)−P(2)−N(2)	118.5(3)	N(2)−P(2)−N(2)#1	115.79(15)	N(2)−P(2)−N(2)#1	115.40(15)	N(3)−P(1)−N(1)	115.37(18)
		N(3)−P(3)−N(4)	116.14(12)	N(4)−P(3)−N(3)	116.49(11)	N(2)−P(3)−N(3)	115.87(18)
		N(3)−P(4)−N(3)#2	115.21(16)	N(4)−P(4)−N(4)#1	115.44(15)	N(6)−P(4)−N(4)	115.60(19)
						N(5)−P(5)−N(4)	116.11(19)
						N(6)−P(6)−N(5)	115.51(19)

[a] Ref 23.

are below and above the plane of the remaining ring atoms (Figure 1 b). The nitrogen atom bound to MX_3 is bent away from this plane (dihedral angles are $AlCl_3$: 19.7° and 17.5°; $AlBr_3$: 21.2° and 19.3°; $GaCl_3$: 21.6° and 20.0°) to a greater extent than the opposite phosphorus atom (dihedral angles are $AlCl_3$: 11.3° and 3.5°; $AlBr_3$: 13.8° and 11.5°; $GaCl_3$: 7.8° and 13.9°). Because of the large difference of the latter dihedral angle for the two molecules of $[PCl_2N]_3 \cdot AlCl_3$ and the two

dx.doi.org/10.1021/ic201075z |Inorg. Chem. 2011, 50, 8937–8945

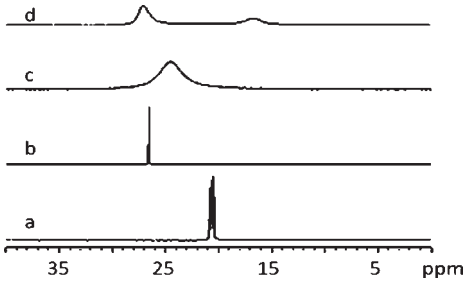

Figure 2. ^{31}P NMR spectra at 25 °C in C_6D_6 (a) $[PCl_2{}^{15}N]_3$, (b) $[PCl_2{}^{15}N]_3 \cdot GaCl_3$, (c) $[PCl_2{}^{15}N]_3 \cdot AlCl_3$, and (d) $[PCl_2{}^{15}N]_3 \cdot AlBr_3$.

molecules of $[PCl_2N]_3 \cdot GaCl_3$, packing forces would appear to be at least partially responsible for the ring bending.

In other ways, the structures of the three $[PCl_2N]_3 \cdot MX_3$ adducts are similar. The distribution of multiple bond character in the rings of $[PCl_2N]_3 \cdot MX_3$ is more accurately shown in eq 1 than in drawing **3**. The P−N bonds that flank the M−N bond show single bond character, both at 1.6521(14) Å in $[PCl_2N]_3 \cdot AlCl_3$, both at 1.6532(15) in $[PCl_2N]_3 \cdot AlBr_3$, and ranging from 1.648(3) to 1.650(3)Å (average = 1.649 Å) in $[PCl_2N]_3 \cdot GaCl_3$. The remaining P−N bonds show multiple bond character ranging 1.561(2)−1.572(2) Å (avg. 1.567 Å) for $[PCl_2N]_3 \cdot AlCl_3$, 1.562(2)−1.575(2) Å (average = 1.569 Å) for $[PCl_2N]_3 \cdot AlBr_3$, and 1.566(4)−1.576(3) Å (avg. = 1.570 Å) for $[PCl_2N]_3 \cdot GaCl_3$. Though there may be a slight alternation in the multiply bonded P−N distances, the values are all within experimental error of one another. These distances are similar to those in $[PCl_2N]_3$ (1.5795(16)−1.5822(17) Å, average = 1.581 Å[23]). The P−N−P angle at the nitrogen atom bound to MX_3 (all within 1.1° of 117.1°) is smaller than the P−N−P angles at the free nitrogen atoms in the adducts (all within 1.1° of 124.5°) or in the free ring (average = 121.2°[23]). All N−P−N angles in the three adducts (all within 0.8° of 115.9°) decrease ∼2° from those in the free ring (average = 118.41°).[23] Similar changes in ring geometry to those described above have been observed for adducts of $[PCl_2N]_3$ and other phosphazene rings.[6,12,24]

NMR Studies. The NMR studies were carried out on both $[PCl_2{}^{15}N]_3 \cdot MX_3$ and $[PCl_2N]_3 \cdot MX_3$. The unlabeled species provided spectra that were easier to model, whereas the ^{15}N labeled species allowed for more detailed characterization through multinuclear NMR studies. Figure 2 shows the ^{31}P NMR spectra of the three $[PCl_2{}^{15}N]_3 \cdot MX_3$ adducts and that of $[PCl_2{}^{15}N]_3$ in C_6D_6 solution at 25 °C. The spectral data of $[PCl_2{}^{15}N]_3 \cdot MX_3$ are consistent with fluxional structures. The ^{31}P chemical shifts of the adducts differ by no more than 7 ppm from the resonance for $[PCl_2{}^{15}N]_3$ at 20.6 ppm.[25] Only the spectrum of $[PCl_2{}^{15}N]_3 \cdot AlBr_3$ shows the two resonances expected for a static adduct, but the broadness of the spectrum indicates that an exchange process is taking place. The exchange is fastest in the case $[PCl_2{}^{15}N]_3 \cdot GaCl_3$, as evidenced by the sharp singlet resonance.

To study the fluxionality of the adducts without the added complications of higher order coupling effects, ^{31}P variable-temperature (VT) NMR spectra of unlabeled adducts were obtained. Figure 3 shows the ^{31}P VT NMR spectra of $[PCl_2N]_3 \cdot AlBr_3$ in $CDCl_3$ obtained at 25 °C, 0 °C, −20 °C, and −40 °C. The numbering scheme for the atoms in the crystal structure (Figure 1) will be used to explain the NMR spectra. At

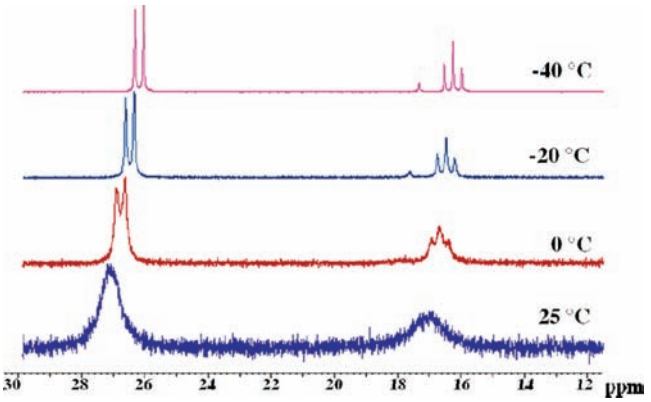

Figure 3. ^{31}P VT NMR spectra of $[PCl_2N]_3 \cdot AlBr_3$ in $CDCl_3$ taken between −40 and 25 °C. The singlet at ∼18 ppm is due to an impurity.

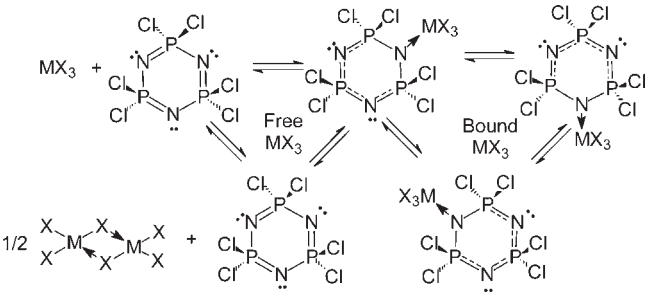

Figure 4. Possible scenarios for the fluxionality of $[PCl_2N]_3 \cdot MX_3$.

25 °C, two resonances at 27.1 ppm for P(1) and P(1A) and 16.9 ppm for P(2) were observed. However, the rate of exchange was greater than the coupling constant, and no coupling was observed. The J-coupling starts to appear at 0 °C. The resonance at 26.7 ppm became a doublet, and the resonance at 16.7 ppm became a triplet. The exchange was slow at −20 °C, and all the expected J-coupling were observed with a well-resolved doublet at 26.5 ppm and a triplet at 16.5 ppm along with a singlet at 17.6 ppm. At −40 °C, the doublet was seen at 26.2 ppm, whereas the triplet was at 16.2 ppm and the singlet was at 17.3 ppm. The singlet was due to protonated impurities in the product. ^{31}P VT NMR spectra of $[PCl_2N]_3 \cdot AlCl_3$ and $[PCl_2N]_3 \cdot GaCl_3$ are shown in the Supporting Information. $[PCl_2N]_3 \cdot AlCl_3$ and $[PCl_2N]_3 \cdot GaCl_3$ showed similar dynamic behavior to that of $[PCl_2N]_3 \cdot AlBr_3$, although the exchange process of $[PCl_2N]_3 \cdot GaCl_3$ was found to be faster than those of $[PCl_2N]_3 \cdot AlCl_3$ and $[PCl_2N]_3 \cdot AlBr_3$.

A saturation transfer study of the ^{31}P NMR spectrum of $[PCl_2N]_3 \cdot AlCl_3$ was carried out to determine whether the singlet due to the impurity was involved in the exchange process. Selectively saturating the doublet resonance in the ^{31}P NMR spectrum of $[PCl_2N]_3 \cdot AlCl_3$ at −20 °C resulted in the saturation of the triplet resonance but had no effect on the singlet resonance. This showed that the doublet and the triplet resonances of $[PCl_2N]_3 \cdot AlCl_3$ are involved in the exchange process, whereas the singlet resonance of the impurity is not.

Classically, fluxionality in MX_3-base adducts occurs by dissociation of the MX_3 from the base.[26] MX_3 as the monomer or dimer can reassociate with the base. This *inter*molecular process is shown in Figure 4 as the free MX_3 route. The saturation

dx.doi.org/10.1021/ic201075z |*Inorg. Chem.* 2011, 50, 8937–8945

transfer study described above suggested that the exchange process may be *intra*molecular. Because $[PCl_2N]_3$ has three nitrogen sites, exchange could be due to movement of MX_3 among the three sites in an *intra*molecular process. This is shown in Figure 4 as the bound MX_3 route. In addition, it would be expected that the energy involved in the exchange process for the free MX_3 route should be significantly greater than that of the bound MX_3 route. In order to distinguish between the possibilities, activation parameters of the $[PCl_2N]_3 \cdot MX_3$ exchange system were obtained.

To derive the activation parameters of the $[PCl_2N]_3 \cdot MX_3$ exchange systems, band shape analyses were performed of the ^{31}P variable-temperature (VT) NMR spectra of the systems.[27] WinDNMR software[28] was used for simulating the ^{31}P VT NMR spectra of all three $[PCl_2N]_3 \cdot MX_3$, and the rate constants of the exchange were obtained at various temperatures. A typical example of the simulation is given in Figure 5. Tables showing the rate constants at various temperatures for $[PCl_2N]_3 \cdot MX_3$ are given in the Supporting Information. Arrhenius plots and plots of $\ln(k/T)$ vs $1/T$ using the rate constants gave the activation parameters for the $[PCl_2N]_3 \cdot MX_3$ systems. Arrhenius plots and plots of $\ln(k/T)$ vs $1/T$ of $[PCl_2N]_3 \cdot AlBr_3$ are shown in Figure 6, and similar plots for $[PCl_2N]_3 \cdot AlCl_3$ and $[PCl_2N]_3 \cdot GaCl_3$ are given in the Supporting Information.

Calculated activation parameters of $[PCl_2N]_3 \cdot MX_3$ in $CDCl_3$ solution are listed in Table 3. The values of E_a, $\Delta H^{\ddagger}$, and $\Delta G^{\ddagger}$ in Table 3 are low and roughly comparable to a hydrogen bond. The $\Delta H^{\ddagger}$ values in Table 3 are about four times smaller than those reported for the complete dissociation of MX_3 complexes of amines and pyridines and those computed for complete dissociation of $[PH_2N]_3 \cdot AlF_3$ and $[P(OH)_2N]_3 \cdot AlF_3$.[26,22] In agreement with the saturation transfer experiment, these values suggest that the exchange in $[PCl_2N]_3 \cdot MX_3$ is taking place through the *intra*molecular-bound MX_3 scenario rather than through complete dissociation of the adduct (Figure 4). It is not clear whether MX_3 can move directly from one nitrogen site to another of the $[PCl_2N]_3$ ring or whether MX_3 binds to one or more lone pairs on the chlorine atoms as it travels between the different nitrogen sites. As expected on the basis of their Lewis acidity toward hard donors,[26] ΔH values follow the sequence $AlCl_3 > AlBr_3 > GaCl_3$.

The results from the above NMR spectral studies for $[PCl_2N]_3 \cdot MX_3$ can be compared to those of other adducts of $[PCl_2N]_3$ and to studies of MX_3 adducts of borazines. Though activation parameters of exchange for adducts other than $[PCl_2N]_3 \cdot MX_3$ have not been obtained, it appears that qualitatively the rate of exchange is in the order $Me^+ \approx SiR_3^+ < AlCl_3 < AlBr_3 < GaCl_3 < Ag^+ \approx H^+$, with only Me^+ and SiR_3^+ showing static structures in solution.[6,12] An intramolecular exchange process in which the Lewis acid moves among the three Lewis basic sites also was proposed to account for the solution fluxionality of $[RBNR']_3 \cdot MX_3$ (MX_3 = $AlBr_3$ and $GaCl_3$).[29] It should be noted that $[PCl_2N]_3 \cdot MX_3$ and $[RBNR']_3 \cdot MX_3$ have somewhat different structures. MX_3 resides roughly in the plane of the $[PCl_2N]_3$ ring in $[PCl_2N]_3 \cdot MX_3$, whereas $AlBr_3$ is above the plane of the $[RBNR']_3$ ring and is bound to the π-type system.[29,30]

The ^{15}N NMR spectra in C_6D_6 of $[PCl_2{}^{15}N]_3 \cdot MX_3$ showed complex signals at 97.3, 93.3, and 95.9 ppm for $AlCl_3$, $AlBr_3$, and $GaCl_3$, respectively, all less than 7 ppm upfield from the resonance of $[PCl_2{}^{15}N]_3$. The ^{27}Al NMR spectra of $[PCl_2{}^{15}N]_3 \cdot AlCl_3$ and $[PCl_2{}^{15}N]_3 \cdot AlBr_3$ showed broad resonances, consistent with efficient quadrupolar relaxation at 107.1 ppm ($\Delta\upsilon_{1/2}$ = 662 Hz)

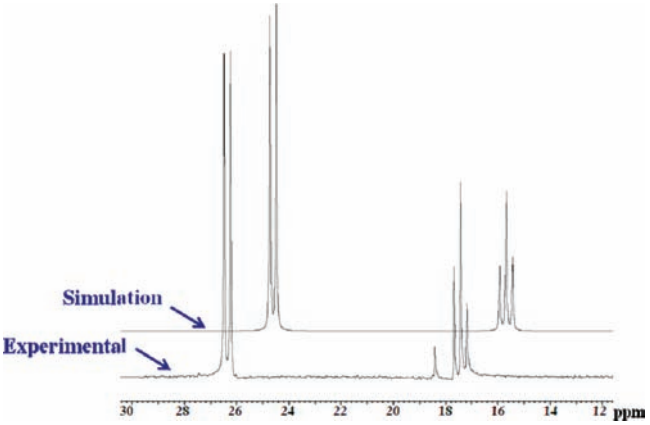

Figure 5. Simulation of ^{31}P NMR spectrum of $[PCl_2N]_3 \cdot AlBr_3$ at −40 °C in $CDCl_3$ by WinDNMR Software. For clarity, the simulated spectrum is offset by about 2 ppm. The simulated spectrum was obtained with a rate constant of 6.

Table 3. Calculated Activation Parameters of the $[PCl_2N]_3 \cdot MX_3$ Exchange in $CDCl_3$

	$[PCl_2N]_3 \cdot AlCl_3$	$[PCl_2N]_3 \cdot AlBr_3$	$[PCl_2N]_3 \cdot GaCl_3$
E_a (kJ mol^{-1} K^{-1})	45.7	40.4	36.8
$\Delta H^{\ddagger}$ (kJ mol^{-1} K^{-1})	43.3	38.3	34.6
$\Delta S^{\ddagger}$ (J mol^{-1} K^{-1})	−55.7	−61.3	−52.8
$\Delta G^{\ddagger}$ (kJ mol^{-1} K^{-1})	59.9	56.5	50.4

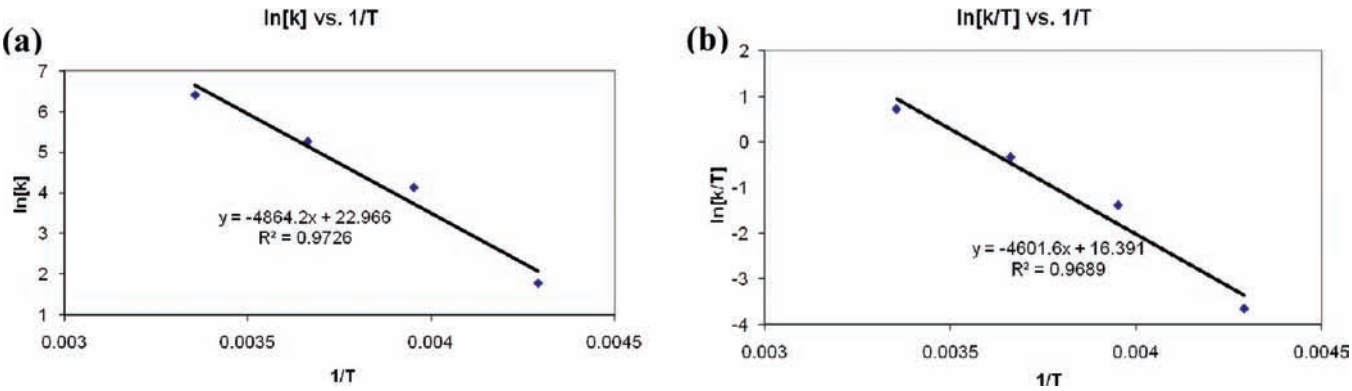

Figure 6. (a) Plot of $\ln[k]$ vs $1/T$ of $[PCl_2N]_3 \cdot AlBr_3$ and (b) plot of $\ln(k/T)$ vs $1/T$ of $[PCl_2N]_3 \cdot AlBr_3$.

dx.doi.org/10.1021/ic201075z |*Inorg. Chem.* 2011, 50, 8937–8945

and 94.0 ppm ($\Delta\upsilon_{1/2}$ = 423 Hz), which are shifted downfield ~7 and ~14 ppm from the signal of $(AlX_3)_2$ (X = Cl, Br), respectively. The ^{27}Al chemical shifts are consistent with four-coordinate centers.

The ^{31}P VT NMR spectra of $[PCl_2{}^{15}N]_3 \cdot AlBr_3$ in CD_2Cl_2 are shown in Figure 7, and such spectra for $[PCl_2{}^{15}N]_3 \cdot AlCl_3$ and $[PCl_2{}^{15}N]_3 \cdot GaCl_3$ are shown in the Supporting Information. As in C_6D_6, at 25 °C the exchange in CD_2Cl_2 is slow enough to give two separate resonances. The J-couplings start to appear at 0 °C.

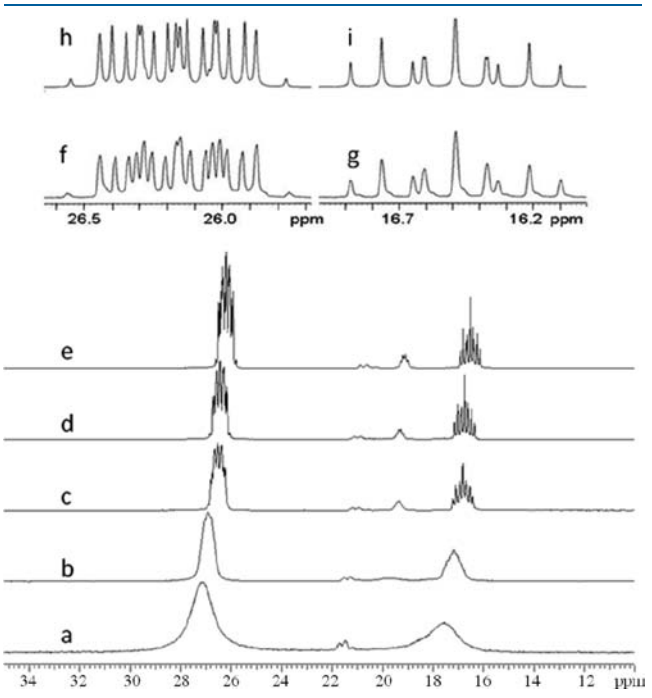

Figure 7. ^{31}P VT NMR spectra of $[PCl_2{}^{15}N]_3 \cdot AlBr_3$ in CD_2Cl_2 taken at 25, 0, −20, −40, and −60 °C (a−e). The downfield signal is assigned to the ^{31}P nuclei nearest to the $AlBr_3$ and the upfield signal to the ^{31}P nuclei furthest from the $AlBr_3$. The smaller signals are assigned to $[PCl_2{}^{15}N]_3 \cdot HAlBr_4$ and free $[PCl_2{}^{15}N]_3$. The traces f and g are the expansions of the two major resonances at −60 °C at 26.2 (f) and 16.5 (g) ppm. Expansions of the regions from the simulated spectrum −60 °C are shown as traces (h) and (i) (A 1.5 Hz line width is imposed on the simulated spectrum).

At −60 °C, the exchange slows in comparison to the small J coupling on the NMR time scale to show complex splitting patterns: an AA′MXX′Y pattern is observed for P(1)/P(1A) at 26.2 ppm (XX′Y are the ^{15}N atoms). A pair of weak signals in the wings of this multiplet (near 26.55 and 25.75 ppm) are evidence of these higher order coupling effects and a triplet of triplets for P(2) at 16.5 ppm. These couplings are consistent with the formulation $[PCl_2{}^{15}N]_3 \cdot AlBr_3$. Weaker resonances due to free $[PCl_2{}^{15}N]_3$ and $[PCl_2{}^{15}N]_3 \cdot HAlBr_4$ are also observed in the spectra.

In order to correctly assign all coupling constants for the $[PCl_2{}^{15}N]_3 \cdot AlBr_3$ adduct, a ^{31}P−^{31}P homonuclear (two-dimensional) 2DJ spectrum was obtained at −60 °C. Expansions of the resonances for P(1)/P(1A) and P(2) are shown in Figure 8. On the basis of Figure 8, the 16 peak multiplet at 26.2 ppm in Figure 7 for P(1) is due to a two-bond ^{31}P−^{31}P coupling between (P(1)/P(1A)−P(2)) of 44.5 Hz (along F_1), and two slightly different one-bond ^{31}P−^{15}N couplings of −24.5 Hz (P(1)−N(2)) and −22.5 Hz (P(1)−N(1); the remainder of the cross peaks in panel (a) of Figure 8 (and the extra splitting in the 1D ^{31}P spectrum) arise from strong coupling effects.[31] The slightly larger one-bond ^{31}P−^{15}N coupling is assigned to the shorter P−N bond. The nine peaks for P(2) at 16.5 ppm in Figure 7 are due to a 44.5 Hz two-bond ^{31}P−^{31}P coupling between P(2) and the chemically equivalent P(1) and P(1A) and a one-bond ^{31}P−^{15}N coupling between (P(2) and the chemically equivalent N(2) and N(2A) of −18.8 Hz. For further confirmation, spin simulation was performed using the couplings as they were measured from the 2DJ spectrum. On the basis of prior work on similar compounds, in the spin simulation, the following were assumed: $^2J_{NN}$ and $^3J_{PN}$ were negligible, $^2J_{PP} > 0$,[32,33] $^1J_{PN} < 0$, and the value of $^2J_{P1-P1A}$ was varied (this coupling was not obtainable from direct measurement of spectral features, but optimum results were obtained with $^2J_{P1-P1A}$ = 24.1 Hz).

CONCLUSIONS

Three $[PCl_2N]_3 \cdot MX_3$ adducts have been synthesized from $[PCl_2N]_3$ and MX_3. The $[PCl_2N]_3 \cdot MX_3$ adducts are water and light sensitive, and impurities of $[PCl_2N]_3 \cdot HMX_4$ are difficult to avoid. The adducts have been characterized by their physical properties and X-ray crystallography. VT NMR studies show that

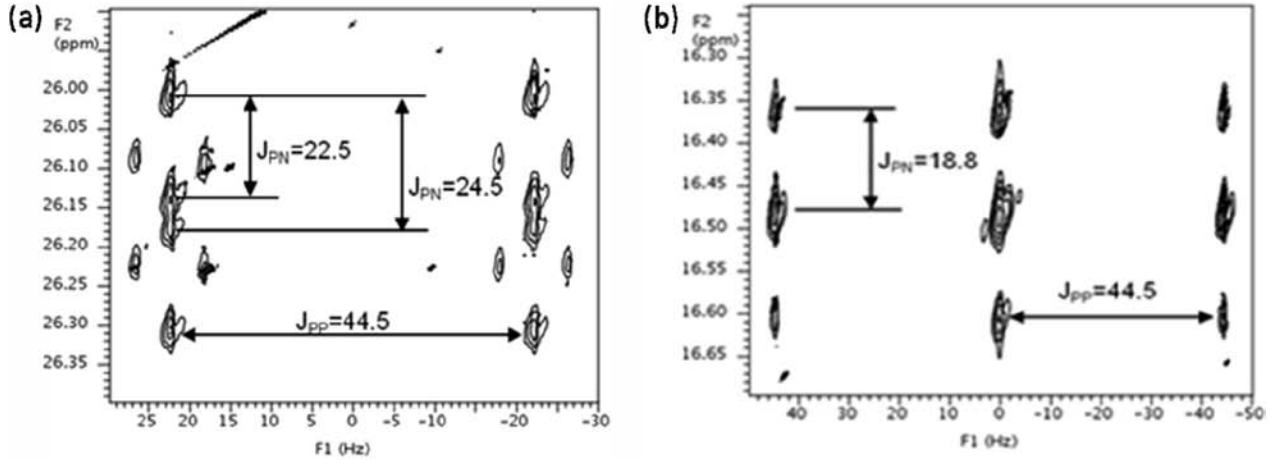

Figure 8. Expansions from the 2D ^{31}P−^{31}P homonuclear 2DJ spectrum of $[PCl_2{}^{15}N]_3 \cdot AlBr_3$ in CD_2Cl_2 at −60 °C showing the two major resonances: (a) ^{31}P nuclei nearest the $AlBr_3$ (P(1) or P(1A)) and (b) ^{31}P nuclei furthest from the $AlBr_3$ (P(2)). The streak in the upper left of the former spectrum is a data processing artifact.

dx.doi.org/10.1021/ic201075z |Inorg. Chem. 2011, 50, 8937–8945

the adducts are fluxional in solution. Calculated activation parameters suggest that the exchange in $[PCl_2N]_3 \cdot MX_3$ is taking place through a scenario in which free MX_3 is not generated. The fragility of $[PCl_2N]_3 \cdot MX_3$ at or near room temperature suggests that such adducts are not involved directly as intermediates in the high-temperature ROP of $[PCl_2N]_3$ to give $[PCl_2N]_n$.

■ ASSOCIATED CONTENT

Supporting Information. Crystallographic and spectral data. This material is available free of charge via the Internet at http://pubs.acs.org.

■ AUTHOR INFORMATION

Corresponding Author
*E-mail: tessier@uakron.edu.

■ ACKNOWLEDGMENT

We thank the National Science Foundation (USA) for support of this work under grants CHE-0316944 and CHE-0616601. We also thank the National Science Foundation and the Ohio Board of Regents for funds used to purchase the NMR (CHE-9977144) and the X-ray diffractometer (CHE-0116041) instruments used in this work. We thank the Goodyear Corporation for donation of an NMR instrument used in this work. We thank R. Newmark of 3M Corporation for helpful discussion with regard to interpretation of the NMR data. We thank John N. Rapko (St. Louis College of Pharmacy, St. Louis, MO) for reading the original manuscript and making valuable suggestions.

■ REFERENCES

(1) Allcock, H. R. *Chemistry and Applications of Polyphosphazenes*; Wiley-Interscience: New York, 2003; Chapters 4 and 5.

(2) Hagnauer, G. L. *J. Macromol. Sci., Chem.* **1981**, *A16*, 385–408.

(3) (a) Emsley, J.; Udy, P. B. *Polymer* **1972**, *I*, 593–594. (b) Sulkowski, W. In *Synthesis and Characterizations of Poly(organophosphazenes)*; Gleria, M., De Jaeger, R., Eds.; Nova Science: New York, 2004; Chapter 4.

(4) Boomishankar, R.; Ledger, J.; Jean-Baptiste Guilbaud, J.-B.; Campbell, N. L.; Bacsa, J.; Bonar-Law, R.; Khimyak, Y. Z.; Steiner, A. *Chem. Commun.* **2007**, 5152–5154.

(5) (a) Kayser Potts, M.; Hagnauer, G. L.; Sennett, M. S.; Davies, G. *Macromolecules* **1989**, *22*, 4235–4239. (b) Sennett, M. S.; Hagnauer, G. L.; Singler, R. E.; Davies, G. *Macromolecules* **1986**, *19*, 959–964.

(6) (a) Zhang, Y.; Tham, F. S.; Reed, C. A. *Inorg. Chem.* **2006**, *45*, 10446–10448. (b) Zhang, Y.; Huynh, K.; Manners, I.; Reed, C. A. *Chem. Commun.* **2008**, 494–496.

(7) (a) Allcock, H. R. *Phosphorus-Nitrogen Compounds*; Academic: New York, 1972; Chapter 10. (b) Bode, H.; Bach, H. *Chem. Ber.* **1942**, *75B*, 215–226. (c) Becke-Goerhring, M.; John, K. Z. *Anorg. Allg. Chem.* **1960**, *304*, 126–136.

(8) Allcock, H. R. *Phosphorus-Nitrogen Compounds*; Academic: New York, 1972; Chapters 4, 10, 11, 12.

(9) (a) Coxon, G. E.; Sowerby, D. B. *J. Chem. Soc. A* **1969**, 3012–3014. (b) Kravchenko, E. A.; Levin, B. V.; Bananyarly, S. I.; Toktomatov, T. A. *Koord. Khim.* **1977**, *3*, 374–379. (c) Becke-Goehring, M.; Hohenschutz, H.; Appel, R. Z. *Naturforsch.* **1954**, *9b*, 678–681. (d) Kandemirli, F. *Phosphorus, Sulfur, Silicon Relat. Elem.* **2003**, *178*, 2331–2342. (e) Hota, N. K.; Harris, R. O. *J. Chem. Soc., Chem. Commun.* **1972**, 407–408. (f) Zhivukhin, S. M.; Kireev, V. V. *Russ. J. Inorg. Chem.* **1964**, *9*, 1439–1440. (g) Derbisher, G. V.; Babaeva, A. V. *Russ. J. Inorg. Chem.* **1965**, *10*, 1194–1195. (h) Baranwal, B. P.; Das, S. S.; Farva, U. *Res. J. Chem. Environ.* **2001**, *5*, 55–58. (i) Bode, H.; Bach, H. *Chem. Ber.* **1942**, *75B*, 215–226.

(10) (a) Bode, H.; Bütow, K.; Lienau, G. *Chem. Ber.* **1948**, *81*, 547–552. (b) Feakins, D.; Last, W. A.; Neemuchwala, N.; Shaw, R. A. *Chem. Ind. (London)* **1963**, 164–165. (c) Sayed, M. B. *Internet J. Chem.* 2002, *5*, Paper No. 6.

(11) (a) Heston, A. J.; Tessier, C. A.; Panzner, M. J.; Youngs, W. J. *Phosphorus, Sulfur Silicon Relat. Elem.* **2004**, *179*, 831–837. (b) Heston, A. J.; Panzner, M. J.; Youngs, W. J.; Tessier, C. A. *Inorg. Chem.* **2005**, *44*, 6518–6520.

(12) Gonsior, M.; Antonijevic, S.; Krossing, I. *Chem.—Eur. J.* **2006**, *12*, 1997–2008.

(13) Shriver, D. F.; Drexdon, M. A. *The Manipulation of Air-Sensitive Compounds*, 2nd ed.; Wiley: New York, 1986.

(14) Plesch, P. H. *High Vacuum Techniques for Chemical Syntheses and Measurements*; Cambridge University Press: New York, 1989.

(15) Sheldrick, G. M. *SHELX97: Programs for Crystal Structural Analysis*; University of Göttingen, Göttingen, Germany, 1997.

(16) Rivard, E.; Lough, A. J.; Chivers, T.; Manners, I. *Inorg. Chem.* **2004**, *43*, 802–811.

(17) Akhrem, I.; Alexander Orlinkov, A. *Chem. Rev.* **2007**, *107*, 2037–2079.

(18) Mirda, D.; Rapp, D.; Kramer, G. M. *J. Org. Chem.* **1979**, *44* (15), 2619–2624.

(19) (a) Several scales of relative Lewis acidity have been proposed: Santelli, M.; Pons, J.-M. *Lewis Acids and Selectivity in Organic Synthesis*; CRC: New York, 1996; Chapter 1. (b) Olah, G. A.; Kobayashi, S.; Tashiro, M. *J. Am. Chem. Soc.* **1972**, *94*, 7448–7461. (c) Kobayashi, S.; Busujima, T.; Nagayama, S. *Chem.—Eur. J.* **2000**, *6*, 3491–3494. (d) Chen, E. Y.-X.; Marks, T. *J. Chem. Rev.* **2000**, *100*, 1391–1434.

(20) (a) Schulz, S. *Adv. Organomet. Chem.* **2003**, *49*, 225–317. (b) Haaland, A. In *Coordination Chemistry of Aluminum*; Robinson, G. H., Ed.; VCH: New York, 1993; pp 1−56. (c) Krossing, I.; Nöth, H.; Schwenk-Kircher, H.; Seifert, T.; Tacke, C. *Eur. J. Inorg. Chem.* **1998**, 1925–1930. (d) Jonas, V.; Frenking, G.; Reetz, M. F. *J. Am. Chem. Soc.* **1994**, *116*, 8741–8753. (e) Haaland, A. *Angew. Chem., Int. Ed. Engl.* **1989**, *28*, 992–1007.

(21) Some recent examples: (a) Nogai, S.; Schwriewer, A.; Schmidbaur, H. *Dalton Trans.* **2003**, 3165–3171. (b) Ogawa, A.; Fujimoto, H. *Inorg. Chem.* **2002**, *41*, 4888–4894. (c) Cheng, Q. M.; Stark, O.; Merz, M.; Fischer, R. A. *J. Chem. Soc., Dalton Trans.* **2002**, 2933–2936. (d) Waltman, R. J.; Lengsfield, B.; Pacansky *J. Chem. Mater.* **1997**, *9*, 2185–2196. (e) Luo, B.; Kucera, B. E.; Gladfelter, W. L. *Chem. Commun.* **2005**, 3463–3465. (f) Carmalt, C. J.; Mileham, J. D.; White, A. J. P.; Williams, D. J. *Dalton Trans.* **2003**, 4255–4260. (g) Tang, C. Y.; Downs, A. J.; Greene, T. M.; Marcahnt, S.; Parsons, S. *Inorg. Chem.* **2005**, *44*, 7143–7150. (h) Tang, C. Y.; Downs, A. J.; Greene; Kettle, L.; Rankin, D. W. H.; Robertson, H. E.; Turner, A. R. *Dalton Trans.* **2006**, 1204–1212. (I) Timoshkin, A. Y.; Bettinger, H. F.; Schaefer, H. F., III *Inorg. Chem.* **2002**, *41*, 738–747.

(22) Waltman, R. J.; Lengsfield, B.; Pacansky, J. *Chem. Mater.* **1997**, *9*, 2185–2196.

(23) (a) Bullen, G. J. *J. Chem. Soc. A* **1971**, 1450–1453. (b) Bartlett, S. W.; Coles, S. J.; Davies, D. B.; Hursthouse, M. B.; Ibisoglu, H.; Kilic, A.; Shaw, R. A.; Un, I. *Acta Crystallogr.* **2006**, *B62*, 321–329.

(24) (a) Chadrasekhar, V.; Venkatasbbaiah, K. In *Applicative Aspects of Cyclophosphazenes*; Gleria, M., De Jaeger, R., Eds.; Nova Science: New York, 2004; Chapter 7 (b) Allen, C. W. In *The Chemistry of Inorganic Homo- and Heterocycles*; Haiduc, I., Sowerby, D. B., Eds.; Academic: New York, 1987; Vol. 2, Chapter 20.

(25) Thomas, B.; Grossmann, G. *J. Magn. Reson.* **1979**, *36*, 333–341.

(26) (a) Tuck, D. In *Chemistry of Aluminium, Gallium, Indium and Thallium*; Downs, A., Ed.; Blackie Academic & Professional: London, 1993; Chapter 8. (b) Davydova, E. I.; Sevastianova, T. N.; Suvorov, A. V.; Timoshkin, A. Y. *Coord. Chem. Rev.* **2010**, *254*, 2031–2077. (c) Haarland, A. In *Coordination Chemistry of Aluminum*; Robinson, G. H., Ed.; VCH: New York, 1993; Chapter 1. (d) Haarland, A. *Angew. Chem., Int. Ed. Engl.* **1989**, *28*, 992–1007.

(27) Sandstrom, J. *Dynamic NMR Spectroscopy*; Academic: New York, 1984; Chapter 6.

(28) Reich, H. J. *WINDNMR: NMR Spectrum Calculations*, version 7.1.13; University of Wisconsin: Madison, WI, 2008.
(29) (a) Anton, K.; Fuβstetter, H.; Nöth, H. *Chem. Ber.* **1981**, *114*, 2723–2730. (b) Anton, K.; Nöth, H. K. *Chem. Ber.* **1982**, *115*, 2668–2673. (c) Gemünd, B.; Günther, B.; Nöth, H. *ARKIVOC* **2008**, *5*, 136–152.
(30) Lisovenko, A.; Timoshkin, A. *Inorg. Chem.* **2010**, *49*, 10357–10369.
(31) Bax, A. *Two-Dimensional Nuclear Magnetic Resonance in Liquids*; Delft University Press: Dordrecht Holland, 1982; pp 116−119.
(32) Krishnamurth, S. S.; Woods, M. *Annu. Rep. NMR Spectrosc.* **1987**, *19*, 175–320.
(33) Thomas, B.; Grossmann, G. *Russ. Chem. Rev.* **1986**, *55*, 622–636.